Technical University of Denmark

DTU

Modelling Human Tibia Structural Vibrations

Thomsen, Jon Juel

[Link back to DTU Orbit](#)

DTU Library
Technical Information Center of Denmark

MODELLING HUMAN TIBIA STRUCTURAL VIBRATIONS

JON JUEL THOMSEN

Department of Solid Mechanics, The Technical University of Denmark, Building 404, DK-2800
Lyngby, Denmark

Abstract—Mode shapes and natural frequencies of human long bones play an important role in the interpretation, prediction and control of their dynamic response to external mechanical loads. This paper describes an experimental and theoretical study of free vibrations in an excised human tibia. Experimentally, seven tibial natural frequencies in the range 0–3 kHz were identified through measured structural transfer functions. Theoretically, a beam type Finite Element model of a human tibia is suggested. Unknown parameters in this model are determined by a Bayesian parameter estimation approach, by which very fine model/observation-accordance was achieved with realistic parameter estimates. A sensitivity analysis of the model confirms that the human tibia in a vibrational sense is more uniform than its complicated geometry would immediately suggest. Accordingly, two simple tibia models are identified, based on uniform beam theory with inclusion of shear deformations.

1. INTRODUCTION

How will a human tibia respond to external dynamic loads? This question arises naturally in conjunction with rather diverse biomechanical problems: development of non-invasive methods of monitoring fracture healing and diagnosis of bone diseases, assessment of bone stresses under normal or extreme conditions, simulation of human gross motion and construction of experimental dummies.

To answer the question, an adequate mathematical model would be of great importance. Such a model could provide a deeper understanding of experimental observations and perhaps replace experiments in situations where such would be unethical, very costly or impossible to perform.

Scientific interest in bone mechanics has a long tradition, Galileo (1638) being a pioneer and works of Bourgery (1832), Koch (1917) and Wolff (1870) being important cornerstones. Early efforts were primarily concerned with experimental studies of statical bone properties. However, the past two decades have shown significant progress in the field of mathematical bone modelling owing to the ability of powerful numerical methods in connection with developments in computer technology, to handle the complex, irregular geometry of most bones. Parallel to this, developments in experimental methods and instrumentation meant that theoretical model predictions could also be verified experimentally. These tools have given rise to a considerable amount of studies dealing with statical properties of bones (cf. Evans, 1973; King, 1984; Huiskes and Chao, 1983) and a more limited number of studies concerning dynamical models of bones.

Concentrating on dynamical modelling, Viano *et al.* (1986) proposed a non-uniform beam model of a human femur shaft, using 10 Timoshenko beam ele-

ments and assuming one isotropic bone material (compact bone). Unknown material parameters were determined by matching the lowest natural frequencies predicted by the model to natural frequencies observed experimentally by Michelson interferometry. By allowing different material parameters for different types of vibration, good accordance could be obtained. Khalil *et al.* (1981) presented a model of a complete human femur, based on 59 Timoshenko beam elements, including both compact and cancellous bone. The lowest 20 natural frequencies of this model were computed and compared with frequencies identified from experimentally measured transfer functions. Excellent agreement (within 3% in average) between theoretical and experimental natural frequencies was noted. In a series of papers, Christensen *et al.* (1986), and Cornelissen *et al.* (1986, 1987) describe several important aspects relating to experimental determination and interpretation of the lowest natural frequencies and mode shapes of human tibiae *in vitro, in situ* and *in vivo*. Of primary concern to this group is the evaluation of a clinical method for non-invasive monitoring of healing fractures. Hight *et al.* (1980) examined the significance of various modelling aspects in connection with a beam element model of a tibia. Assessed were the importance of axis curvature and twist, shear deformations, boundary conditions, and mass formulation. Model predictions were not verified experimentally in this study. Collier *et al.* (1982) used sinus sweep excitation to determine the lowest 5 natural frequencies of an excised human tibia. Experimental frequencies were compared with analytical results obtained by modelling the tibia as a hollow Bernoulli–Euler beam with the constant cross-section of an isosceles triangle. Acceptable model/experiment accordance was obtained for flexural vibrations only by allowing the value of Young's modulus to vary with the direction of excitation.

The study described in the following was concerned with possible improvements within three areas of

dynamic tibia modelling: (1) The frequency range is extended. as short duration impacts may excite higher vibration modes. (2) More attention is paid to shear related modelling aspects, as both torsional modes and flexural high frequency modes are considerably influenced by these. (3) In tuning the solid mechanics model of a tibia to reality, model parameters which have a clear physical interpretation are restricted to values in accordance herewith.

The tibia is mathematically modelled as a straight, twisted non-uniform Timoshenko beam, composed of two linearly elastic and transversely isotropic materials (compact and cancellous bone), and one perfectly flexible material (bone marrow). Unknown parameters in this model are determined by a Bayesian parameter estimation approach, in tuning the model to experimentally determined undamped resonant frequencies of an excised and embalmed human tibia.

2. EXPERIMENTAL DETERMINATION OF TIBIAL RESONANCES

An excised and embalmed human left tibia was supported in two elastic straps simulating free-free supporting conditions, and a standard frequency analysis was made, using averaged frequency response functions determined by impulse hammer excitation (Bendat and Piersol, 1980). The tibial acceleration response was traced by a miniature piezoelectric accelerometer which was mounted on cement studs glued to the tibial surface. A total of 14 combinations of accelerometer and hammer excitation locations were used. These combinations were chosen in order to enhance selectively each of the fundamental types of tibial vibration modes: flexural vibration in two planes and torsional and longitudinal vibrations. Response linearity was verified prior to the experiments by varying the input force and noting a proportional increase in output level, and during the experiments by computing and surveying the coherence function associated with each frequency response. The duration of the input impulse was approximately 0.5 ms, providing sufficient excitatory energy in the frequency range of interest (0–4500 Hz), and the acceleration response of the tibia lasted well beyond the duration of this impulse. Examination of the 3 dB bandwidth of the resonance peaks indicated rather low damping ratios (1.7–2.5%), and the peaks were fairly well separated.

Results of an analysis of 14 different frequency response functions, corresponding to different input/ output-locations, are summarized in Table 1. A total of seven undamped natural frequencies in the range 0–2.6 kHz were identified with a high degree of confidence. The frequencies given are obtained by averaging over the number of frequency response functions from which a specific resonance appeared, as, in general, only five or six frequencies were extracted from each frequency response. The standard deviations given relate hereto. Table 1 also lists three

Table 1. Experimentally identified undamped natural frequencies of an excised, unsupported human tibia

Mode number	Undamped resonance frequency (Hz)	Standard deviation (Hz)	Mode type
1	431	1	FML-1
2	520	2	FAP-1
3	1112	4	T-1
4	1220	3	FML-2
5	1489	10	FAP-2
6	2199	23	FML-3
7	2575	68	FAP-3
(8)	3250	—	(L-1, T-2,
(9)	3500	—	FML-4 or
(10)	4300	—	FAP-4)

(FML: Flexural vibration in the medio-lateral direction, FAP: Flexural vibration in the anterior–posterior direction, T: Torsional mode, L: Longitudinal mode.)

natural frequencies identified with some uncertainty from only a few frequency responses in the noisy frequency range 2.6–4.5 kHz. Although no great experimental evidence can be assigned to these latter frequencies, they are interesting in that their existences were, as described in Section 4, predicted through mathematical modelling. As no mode shape analysis software was available, the mode type associated with each resonance peak was estimated by collating the magnitude and spectral distribution of resonant peaks, with elementary beam theory and results from studies similar to the present. As appears from Table 1, the resonances occur in pairs of flexural modes, each pair corresponding to vibration in the plane of least respectively largest stiffness, the first two pairs being separated by a torsional mode.

3. A MATHEMATICAL MODEL OF A VIBRATING TIBIA

The tibia is modelled as a straight, twisted, non-uniform Timoshenko beam, made up of three different materials: compact bone, cancellous bone and bone marrow. Compact bone and cancellous bone are idealized as homogeneous, linearly elastic and transversely isotropic materials (Evans, 1973), while bone marrow is considered homogeneous and completely flexible.

The continuum model of the tibia is expressed through partial differential equations in which the unknowns are the time-varying displacement variables describing the deformational state of the beam axis. Deformations corresponding to flexure in two planes, longitudinal extension and torsion, are considered. These equations are discretized by a conventional finite element procedure, using the 2-node, 12-DOF, constant cross-section Timoshenko beam element described by Przemieniecki (1968). Details concerning this element and its parameters are given in
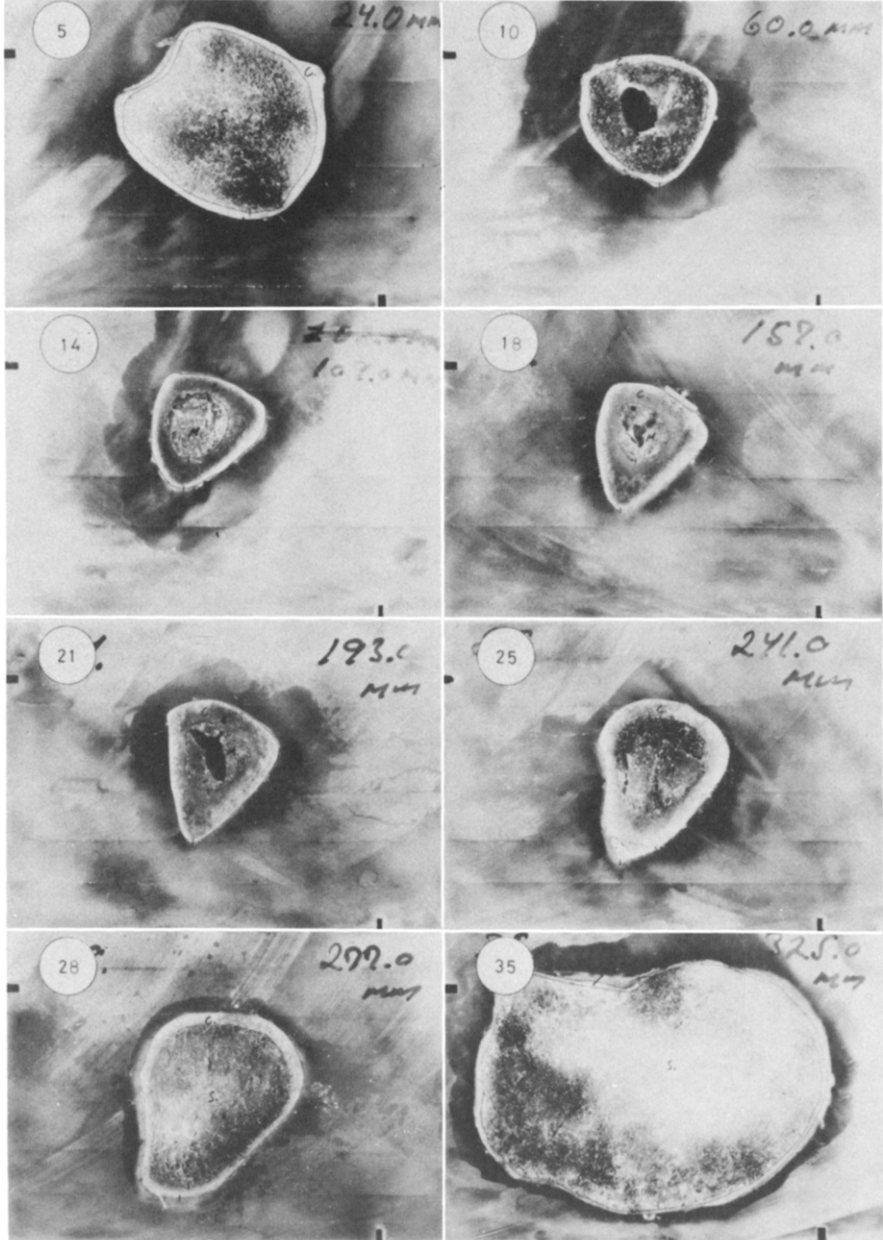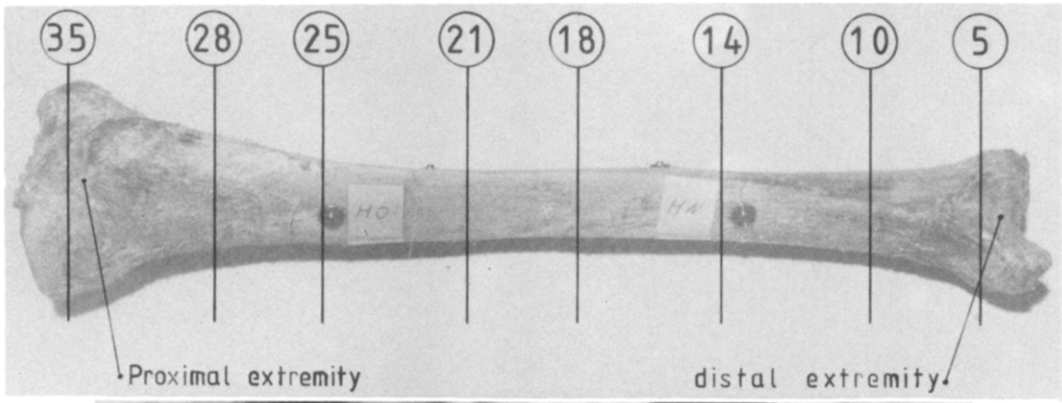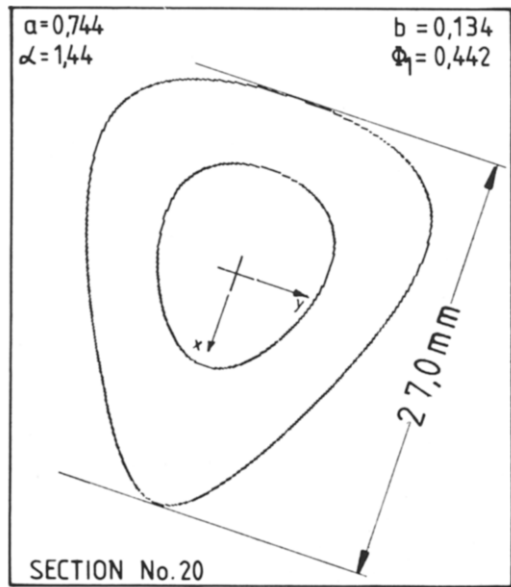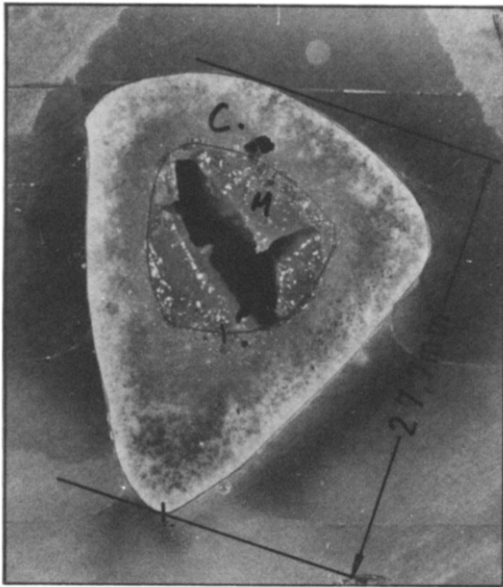
Fig. 1. Typical tibial cross-sections.

217

Fig. 3. A tibial cross-section and its analytical approximation to the expression (5). The two sections have identical bone area, hole area and moments of inertia.

Thomsen (1987). Generally, a tibial section modelled by one beam element consists of three materials: compact bone, cancellous bone and bone marrow. Assuming that the cross-sections of each material have identical centres of area and mass and that no slip occurs on borders to adjacent materials, the stiffness and mass matrix of a tibial section can be obtained by summing element matrices of the three materials in turn. System matrices of the complete tibia are then obtained by assembling coordinate-transformed matrices of individual tibial sections. In the absence of damping and external loads, this leads to the following dynamic equilibrium equations, governing free vibrations of the unsupported tibia:

$$M \cdot \ddot{u} + K \cdot u = 0 \qquad (1)$$

in which M is the system mass matrix, K is the system stiffness matrix, and $u = u(t)$ is the time-varying translations and rotations of element nodes. The corresponding eigenvalue problem is:

$$(K - \omega^2 \cdot M) \cdot \phi = 0 \qquad (2)$$

where ω^2 is an eigenvalue (squared, undamped natural frequency), and ϕ the associated eigenvector (mode shape). Numerical solutions (ω_i, ϕ_i), $i = 1, \ldots, n$ to this problem were obtained by Subspace Iterations (see e.g. Bathe and Wilson, 1976).

Solution accuracy and convergence properties of the finite element code were carefully examined through tests on structural problems for which analytical solutions were available. On this basis, 37 beam elements were assessed sufficiently to make the computational solution error of the tibial problem substantially less than the experimental errors. Each beam element is entirely described by 32 parameters characterizing material and geometry. Material parameters are: Young's modulus E_j, shear modulus G_j,

and density ρ_j, where subscript j refers to type of material: $1 = $ compact bone, $2 = $ cancellous bone, $3 = $ bone marrow. Geometrical parameters are: element length l, axial element position X_0, cross-sectional area A_j, principal moments of inertia I_j^I, I_j^{II}, rotation of principal axes θ_j, Timoshenko shear coefficients k_j^I, k_j^{II} and torsional stiffness factor K_j. Parameters characterizing material are assumed to be constant along the tibial axis. Moreover, as bone marrow is considered perfectly flexible (i.e. $E_3 = G_3 = 0$), the tibial material is fully described through seven parameters $(E_{1,2}, G_{1,2}, \rho_{1,2,3})$. Their determination is described in a following section.

Geometrical parameters were obtained by digitizing the geometry of the tibia on which the dynamic measurements were actually performed. The tibia was cast in epoxy and sliced into 38 transverse sections, the distance between cuts being 6 mm at the extremities, 12 mm at the shaft. Typical cross-sections are shown in Fig. 1. Each section was photographed and enlarged, and the cross-sectional border curves of compact bone, cancellous bone and bone marrow were digitized using an electronic pencil. The digitized points were connected by means of cubical splines, and the resulting cross-section representations were analysed using CAD CAE-software (I-DEAS, 1986). Detailed analysis results, consisting of numerical values of cross-sectional centroids, areas and moments of inertia of the three materials in 38 sections, are given in Thomsen (1987). Here, only the cross-sectional area distribution along the tibial axis is shown (Fig. 2). A plot of the tibial centroid trajectory justified the assumption of a straight neutral axis as the absolute deviation from a straight line was, in mean, only 2% of the midshaft diameter. Plots of the variation in principal moments of inertia revealed that the flexural principal plane was nearly parallel to the posterior
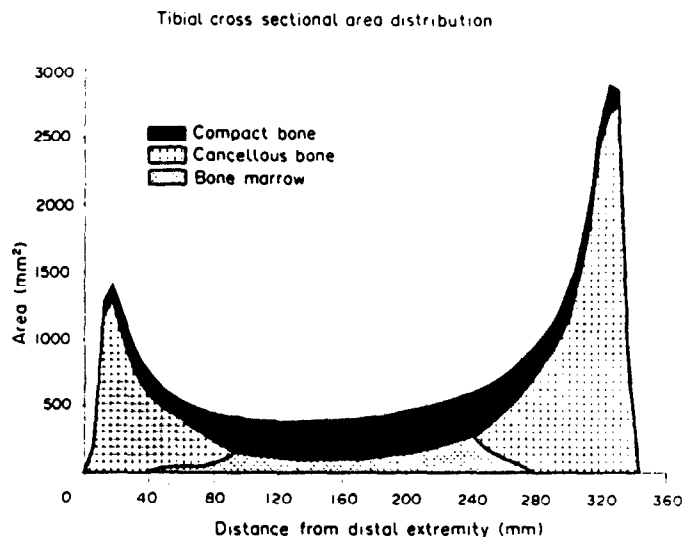
Tibial cross sectional area distribution

Fig. 2. Material distribution along the tibial axis.

surface of the shaft, which implies that the tibia is stiffest in the direction of normal gait. However, differences in the two moments of inertia were moderate, at the distal extremity practically vanishing, which is consistent with the experimental observations of well-defined pairs of flexural natural frequencies.

In similar studies on human femurs (Viano et al., 1986; Khalil et al., 1981), the torsional stiffness factor K has been computed by assuming a constant value of K/J along the bone axis (J is polar inertia). Concerning the tibia, this could hardly be justified, as the cross-sectional geometry exhibits substantial changes from the midshaft (thick-walled isosceles triangle) to the extremities (thin-walled ellipses). This was also a conclusion in the study (Collier et al., 1982) in which the predicted first torsional natural frequency of a tibia was in error by 24%, probably due to the same assumption. Consequently, the axial variation of the torsional rigidity is considered in this study. The torsional stiffness factor of a closed cross-section with one hole, located in the x, y-plane, is given by (Sokolnikoff, 1956):

$$K = K_0 - K_1 \qquad (3a)$$

where:

$$K_i = 2 \int [\Phi(x, y) - \Phi_i] \, dA_i, \quad i = 0, 1 \qquad (3b)$$

in which A_0 and A_1 are domains confined by the outer and inner border-curves C_0 and C_1, respectively, while the stress function $\Phi(x, y)$ is the solution of a Poisson type problem:

$$\frac{\partial^2 \Phi}{\partial x^2} + \frac{\partial^2 \Phi}{\partial y^2} = -2 \text{ in } A_0 \backslash A_1 \qquad (4a)$$

$$\Phi(x, y) = \Phi_i = \text{constant on } C_i, i = 0, 1. \qquad (4b)$$

In order to avoid the extensive computational burden of solving this problem numerically for each of the actual cross-sections, a semi-analytical approach was developed. By this, the border-curves C_i of the actual cross-sections were fitted to analytical expressions of the type:

$$C_i: \quad y(x) = \pm y_i(x) \qquad (5a)$$

$$y_i(x) = \sqrt{\left[\frac{(a + bx^3 - \frac{1}{2}x^2) - \frac{1}{2}(1 + \alpha)\Phi_i}{3bx + \frac{1}{2}\alpha} \right]}, \quad i = 0, 1 \qquad (5b)$$

where a, b, α and $\Phi_1 > \Phi_0 = 0$ are tuneable shape and size parameters. The expression (5) has two very desirable properties: First, it approximates the actual border-curves very well, at least where these are nearly semi-symmetrical (see Fig. 3), and secondly, with border-curves C_i so defined, analytical solutions to the problem (4) can easily be found:

$$\Phi(x, y) = \frac{2}{1 + \alpha} [(a + bx^3 - \frac{1}{2}x^2) - (3bx + \frac{1}{2}\alpha)y^2]. \qquad (6)$$

After fitting all 38 cross-sections to expressions of the form (5), the torsional stiffness factors were found by numerical evaluation of the outer integrals of the plane integral in (3). Details of the procedure are given in Thomsen (1987), and the final result is presented in Fig. 4, showing a significant variation of the ratio K/J of compact bone. (Note that $K/J = 1$ corresponds to a circular cross-section).

The proper way of computing the Timoshenko shear coefficients k' and k'' would include plane integration of a flexure function satisfying a Neumann-type problem (see Cowper, 1966). As this problem has certain similarities with the problem discussed above of finding the torsional stiffness factor, it was natural to try to proceed in a similar way, i.e. using analytical border-curve approximations for which the actual Neumann problem becomes analytically tractable. However, by using expressions of the form (5), it turned out that such analytical solutions were only
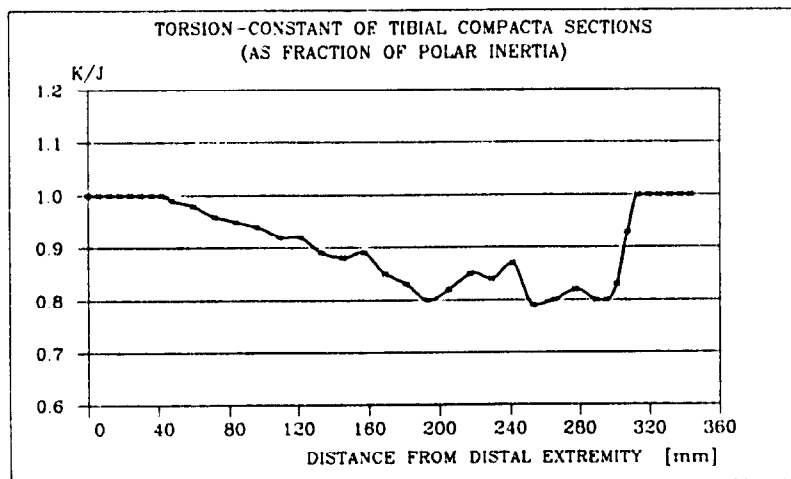

Fig. 4. Torsional stiffness factor K of compact bone. (Normalized by the polar moments of inertia J.)

obtainable in the rather special case of an equilateral triangular cross-section containing incompressible material. Consequently, the more approximate approach of considering each tibial cross-sectional border-curve as circular was used. The shear coefficients of a circular hollow cross-section are given by (Cowper, 1966):

$$k^{\mathrm{I}} = k^{\mathrm{II}} = k = \frac{6(1+v)(1+m^2)^2}{(7+6v)(1+m^2)^2+(20+12v)m^2} \qquad (7a)$$

where v is the Poisson ratio and m is the ratio of inner to outer diameter, which for this purpose is expressed more conveniently through:

$$m^2 \equiv \frac{1-\gamma}{1+\gamma}; \quad \gamma \equiv \frac{A^2}{2\pi J} \qquad (7b)$$

where A is area and J the polar moment of inertia. As the expression for k is rather insensitive to small variations in the Poisson ratio, a value of $v = 0.3$ was chosen as a typical value for both compact and cancellous bone. Results of using (7) on the actual tibial cross-sections are plotted in Fig. 5. At the extremities, the shear coefficient of compact bone cross-sections approaches the value 0.53, which is the theoretical limit value corresponding to a thin-walled tube $(m \rightarrow 1)$. In contrast, the shear coefficient of cancellous bone in these regions is closer to the value 0.89, the theoretical limit value corresponding to a massive circular tube $(m = 0)$. On average, the shear coefficient of compact bone is 0.56, which is close to the constant value 0.55 used by Khalil $et\ al.$ (1981) in their dynamic model of a human femur.

At this stage, the geometry of the tibia is described sufficiently detailed for beam-element modelling. That leaves the determination of material parameters, which is dealt with in the following section.

4. ESTIMATION OF UNKNOWN MODEL PARAMETERS

The model contains seven unknown material parameters: Young's moduli $E_{1,2}$ and shear moduli $G_{1,2}$

of compact and cancellous bone, and the densities $\rho_{1,2,3}$ of compact bone, cancellous bone and bone marrow.

Had the bone materials been fully isotropic, E and G would be interdependent, linked through the Poisson ratio v. As this Poisson ratio could reasonably well be considered as a known parameter, the number of unknown model parameters would thereby be reduced by two (e.g. by eliminating G_1 and G_2). Furthermore, differentiation of the model with respect to unknown model parameters, which is essential to parameter estimation, would be considerably eased, in that E would enter the stiffness matrix of each material as a common factor of all matrix elements.

In fact, the bone materials are considered as only transversely isotropic, implying that, in general, no theoretical relationship exists between E and G. However, given a specific class of structures, here the human tibia, it is reasonable to expect some empirical correlation between those parameters. In fact, Huiskes (1982) used the value $G/E = 0.19$ in a statical analysis of a human femur. We shall here use the value $G/E = 0.23$ for a human tibia, derived from data given in van Buskirk and Ashman (1981). Unknown model parameters are then: Young's moduli $E_{1,2}$ of compact and cancellous bone, and the densities $\rho_{1,2,3}$ of compact bone, cancellous bone and bone marrow.

These five parameters are estimated by minimizing an object function:

$$S(\beta) = (\tilde{f} - f(\beta))^T \cdot V_f^{-1} \cdot (\tilde{f} - f(\beta))$$
$$+ (\tilde{\beta} - \beta)^T \cdot V_\beta^{-1} \cdot (\tilde{\beta} - \beta) \qquad (8)$$

where β is the vector of p unknown parameters, $f(\beta)$ is a vector of n model-predicted natural frequencies, $\tilde{f}$ is a vector of experimentally measured natural frequencies and V_f a covariance matrix of the associated measurement errors. $\tilde{\beta}$ is a vector of subjective a posteriori estimates of the unknown parameters β, and V_β the covariance matrix reflecting the uncertainty in this a posteriori knowledge. The second term of the
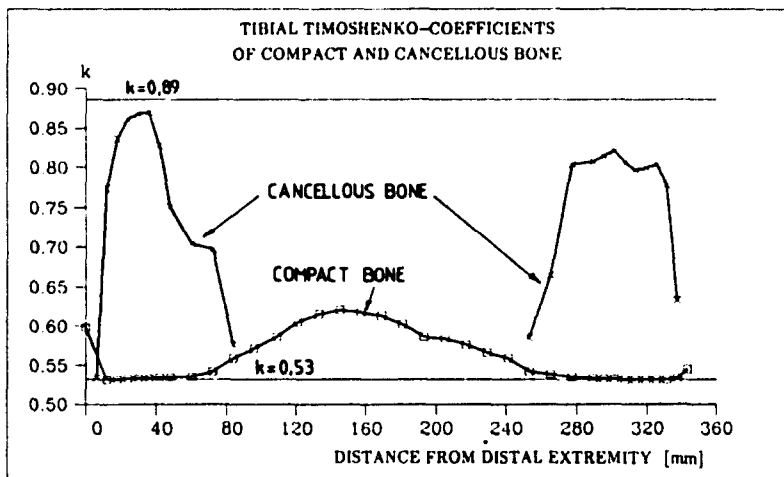

Fig. 5. Timoshenko shear-coefficient k of compact and cancellous bone.

object function (8) makes it a Bayesian estimator, in that prior information regarding the parameters to be estimated are utilized. Besides ensuring that good model/experiment-accordance is not achieved at the expense of completely unrealistic parameter estimates, this second term also makes estimation possible in cases, as the present, where there is no unique set of model parameters which minimizes the first (least square) term of (8) alone.

As the model-frequencies $f(\beta)$ are non-linear in all unknown model-parameters β, the object function must be minimized iteratively. This was done through Gauss–Newton iterations (see e.g. Beck and Arnold, 1977):

$$\beta_{k+1} = \beta_k + P(\beta_k)^{-1} \cdot [X(\beta_k)^T \cdot V_f^{-1} \cdot (\tilde{f} - f(\beta_k))$$
$$+ V_\beta^{-1} \cdot (\tilde{\beta} - \beta_k)] \quad k = 0, 1, \ldots \quad (9)$$

where k is the iteration counter, $X(\beta_k)$ is an n by p sensitivity-matrix with components:

$$X_{ij}(\beta_k) = \left. \frac{\partial f_i}{\partial \beta_j} \right|_{\beta_k} ; \quad i = 1, \ldots, n; \quad j = 1, \ldots, p \quad (10)$$

and the p by p matrix $P(\beta_k)$ is defined through:

$$P(\beta_k) = [X(\beta_k)^T \cdot V_f^{-1} \cdot X(\beta_k) + V_\beta^{-1}] \quad (11)$$

The sensitivity coefficients (10) were obtained as described in the Appendix. The iterations (9) were initiated by the choice $\beta_0 = \tilde{\beta}$. They were terminated when the parameter corrections $|\beta_{k+1} - \beta_k|$ became insignificant. The Gauss–Netwon scheme has fast local convergence properties provided the matrix P is non-singular in the region of minimum. In order to improve the global convergence properties, the Gauss–Netwon scheme was combined with a Back-tracking Linesearch procedure (see e.g. Dennis and Schnabel, 1983).

If P is singular at minimum, the iterations (9) will not converge. If there is no prior information on parameters ($V_\beta^{-1} \to 0$), P is singular if at least two columns in the sensitivity matrix X are linearly dependent. In this case not all parameters can be estimated, although some combinations of parameters probably could be.

Minimization of (8) requires the specification of observations ($\tilde{f}$, V_f) and prior knowledge of parameters ($\tilde{\beta}$, V_β).

The observations $\tilde{f}$ are given by the lowest seven tibial natural frequencies listed in Table 1. Measurement errors were considered to be uncorrelated with zero mean and with variances given by the squared standard deviations of Table 1, i.e.:

$$V_f = \text{Diag}[s_{f_1}^2, s_{f_2}^2, \ldots, s_{f_7}^2] \quad (12)$$

where s_{f_i} are the standard deviations of Table 1, and Diag denotes a diagonal matrix.

The specification of prior knowledge of parameters should reflect the subjective expectation to the parameter values of the tibia in question. This subjective attitude was created by scanning relevant published literature (Evans, 1973; Viano et al., 1986; Khalil et al., 1981; Collier et al., 1982; Huiskes, 1982; van Buskirk and Ashman, 1981; van der Perre and Cornelissen, 1983; Fung, 1981; Chen and Saha, 1987). It was quantified through weighted means of the bone parameters of interest, and through variances reflecting the uncertainty on these subjective expectations. The result is summarized in the first two columns of Table 2. Assuming uncorrelated model parameters, the prior parameter covariances are then given by:

$$V_\beta = \text{Diag}[s_{E_1}^2, s_{E_2}^2, s_{\rho_1}^2, s_{\rho_2}^2, s_{\rho_3}^2]. \quad (13)$$

The iterative estimation process given by (9) converged rapidly and steadily: within three iterations the estimates of E_1 and ρ_1 varied less than 0.01%, while convergence to this variation limit for all five parameters required eight iterations. The resulting estimates were not altered by varying the initial parameter-guesses β_0 by as much as 100%, indicating that a global minimum of (8) was localized. Resulting parameter estimates are given in the third column of Table 2. Note that all parameter estimates are 'realistic', i.e. in accordance with the prior expectation. In fact, this is a consequence of the estimator used.

In the last column of Table 2 crude estimates of the associated parameter estimating errors are given, based on the following linear approximation to the covariance matrix of converged parameter estimates (Beck and Arnold, 1977):

$$\text{Cov}(\beta_{est}) = P^{-1}(\beta_{est}) \quad (14)$$

where β_{est} are parameter estimates and P is defined by (11). Estimation errors computed this way should not be interpreted as errors with respect to true physical parameters, but merely as a measure of the variation in parameter estimates that would appear if the observations $\tilde{f}$ were varied in accordance with their postulated error distribution V_f.

In Table 3, the experimentally measured tibial natural frequencies are compared with the theoretically predicted frequencies based on estimated model parameters. The relative deviations are small and apparently random in sign. Furthermore, their magnitudes are in accordance with the estimated measurement errors, i.e. the largest model/experiment-devi-

Table 2. Identification of tibial model parameters

Model parameter	Prior expectation		Identification results	
	$\tilde{\beta}$	$s_{\tilde{\beta}}$	β	s_β
E_1 (GPa)	20.0	1.0	16.4	0.6
E_2 (GPa)	0.27	0.11	0.12	0.11
ρ_1 (kg m^{-3})	2000	100	2254	85
ρ_2 (kg m^{-3})	850	200	597	41
ρ_3 (kg m^{-3})	1000	200	1227	110

$\tilde{\beta}$: subjective prior expectation, $s_{\tilde{\beta}}$: uncertainty associated herewith (standard deviation), β: identified parameter value based on both prior expectation and experimental observations, s_β: rough estimate of post-identification parameter uncertainty.

Table 3. Comparison of experimentally measured and theoretically computed tibial resonant frequencies (mode type notation: see Table 1)

Mode	Measured natural frequency f_i(Hz)	Theoretical natural frequency f_i (β_{ed}) (Hz)	Deviate (%)
FML-1	431	430	−0.2
FAP-1	520	518	−0.4
T-1	1112	1113	0.1
FML-2	1220	1226	0.5
FAP-2	1489	1429	−4
FML-3	2199	2326	6
FML-3	2575	2638	2

ations are associated with the highest natural frequencies, as are also the measurement errors. This is also a consequence of the estimation procedure used.

The generally fine model/observation accordance, obtained by using realistic values of model parameters, lends credence to the mathematical model. Particularly noteworthy is the small response error of the troublesome torsional natural frequency $T-1$, which, in studies by Collier et al. (1982) and Khalil et al. (1981) were in error by 24% and 10%, respectively. This can probably be partly explained by the special attention paid to shear-related model parameters in the present study.

Using estimated model parameters, higher tibial natural frequencies can be predicted by the mathematical model. Figure 6 shows the model-computed mode shapes of 11 natural frequencies below 4 kHz. The frequency range includes four pairs of flexural modes, two torsional modes and a single longitudinal mode. Only the first seven modes correspond to measured natural frequencies used in the parameter identification. Note, however, that the model-predicted natural frequencies at 3267 Hz (L-1) and 3535 Hz (FML-4) correspond remarkably well to the measured frequencies 3250 Hz and 3500 Hz (Table 1). The latter pair were not used in the parameter identification because of large measurement noise in the high frequency range.

In Fig. 7, an overview of the spectral distribution of the tibial natural frequencies below 5.2 kHz is given. In the shaded spectral region, theoretical model computations are supported by experimental observations. Beyond this region, the points shown must be viewed as purely theoretical model predictions of higher natural frequencies.

In view of the very high consonance between model predictions and experimental observations, made possible by physically realistic model parameters, it is believed that the suggested tibia model incorporates the physical aspects that are of primary importance to correct modelling of at least the lowest seven natural modes of an excised human tibia.

The suggested model probably also contains some physical aspects that are not of primary importance. This is the subject of the following section.

5. A SIMPLE MODEL OF A HUMAN TIBIA

The human tibia is a fairly complex structure. Nevertheless, its resonance spectrum (Fig. 7) and mode shapes (Fig. 6) turned out to be remarkably simple and strongly systematic. Such dynamic characteristics could probably be reproduced by a far more simple mathematical model than the detailed finite element model described above. In fact, modelling human long bones as uniform Bernoulli Euler beams has been proposed by several authors (Collier et al., 1982; Khalil et al., 1981). However, none of these models can be matched to the experimental results of the present study without using highly unrealistic model parameters.

In search of a simple, yet adequate, mathematical model, the detailed Finite Element model was evaluated using several simplifying modelling assumptions. The purpose was a model reduction which would reduce substantially the amount of numerical computation without sacrificing any modelling aspects of primary importance. The following independent model reductions were evaluated:

(a) Neglecting the stiffness of cancellous bone.

(b) Neglecting the mass of bone marrow.

(c) Neglecting the twist of tibial principal planes.

(d) Neglecting shear deformations in flexure.

(e) Neglecting rotational inertia in flexure.

(f) Uniform Timoshenko beam. Cross-sectional parameters based on tibial mid-shaft.

(g) Uniform Timoshenko beam. Cross-sectional parameters based on averaging on the middlemost 3/5 tibial shaft. The influence of cancellous bone at the proximal extremity is simulated by a concentrated mass.

Concentrating first on flexural vibrations only, these model reductions changed the theoretically predicted tibial resonance spectrum as depicted in Fig. 8. Using spectral changes as a measure of model degeneration, the following conclusions were drawn:

(a) The stiffness of cancellous bone can be neglected, as none of the lowest six flexural natural frequencies hereby is changed by more than 0.6%. The distribution of cancellous bone is heavily concentrated at the tibial extremities, especially the proximal. Its mass cannot be neglected as this changes the frequencies by as much as 19–38% (not shown in Fig. 8). Consequently, in a simple model, the influence of cancellous bone should be simulated by concentrated point masses at the extremities.

(b) The influence of bone marrow mass is not insignificant. When it is neglected, the natural frequencies change by 5–7%. However, it could probably be approximated as a uniform distribution of non-structural mass.

(c) Twist of the tibial shaft axis is almost insignificant (frequency changes: 0.5–1.5%). This also appears

FLEXURAL MODES (FML/FAP)		TORSIONAL (T) &
Medio-Lateral (FML)	Anterior-Posterior (FAP)	LONGITUDINAL (L) MODES
mode FML-1 430 Hz	mode FAP-1 518 Hz	mode T-1 1113 Hz
mode FML-2 1226 Hz	mode FAP-2 1429 Hz	
mode FML-3 2326 Hz	mode FAP-3 2638 Hz	mode T-2 3029 Hz
mode FML-4 3535 Hz	mode FAP-4 3916 Hz	mode L-1 3267 Hz

Fig. 6. Theoretically computed tibial mode shapes.

from the almost de-coupled flexural mode shapes shown in Fig. 8.

(d) Flexural shear deformations cannot be neglected. Doing so implies frequency changes of order 2–18%. This somewhat surprising fact is explained by the following considerations:

— The tibia is not pronouncedly slender: wave lengths of the lowest three pairs of flexural mode
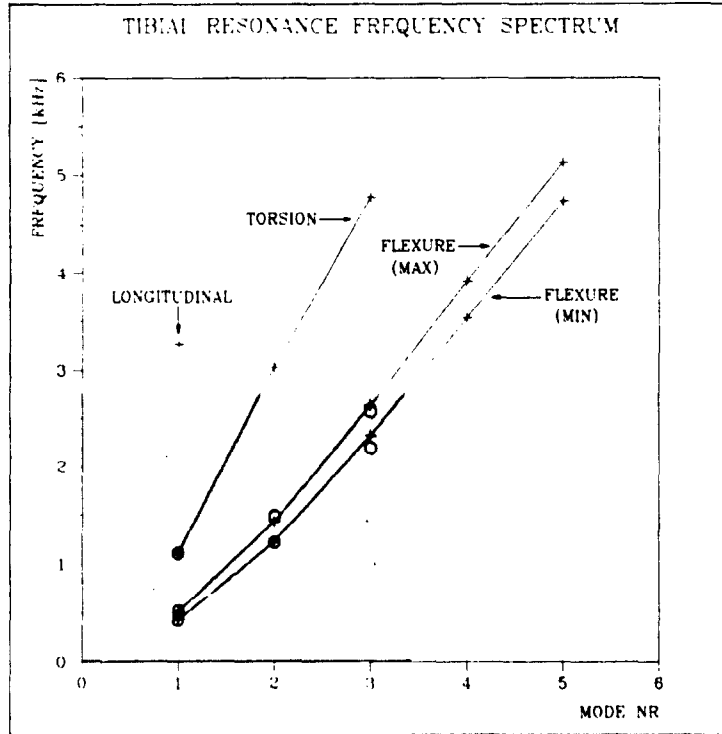
Fig. 7. Tibial resonance spectrum. (+: Model predicted natural frequency. O: Experimentally observed resonance.)
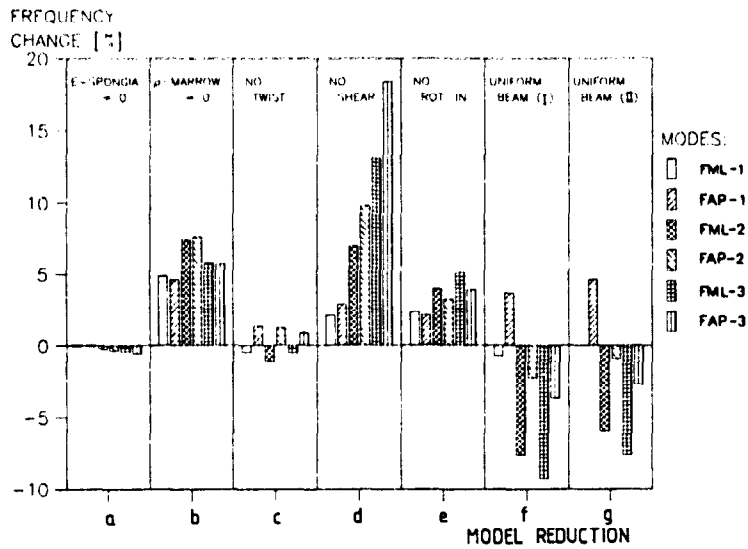

Fig. 8. Changes in model-computed flexural natural frequencies due to several independent model reductions.

shapes are 340 mm, 228 mm and 171 mm, compared with cross-sectional diameters of 20–50 mm.

— The shear modulus of compact bone is low: approximately 40% lower than the corresponding isotropic value [which is $E/2(1 + v)$].

— Except for the mid-shaft region, the bone cross-sections are rather thin-walled. This implies low shear coefficients, which further reduces the shear stiffness.

Consequently, the influence of flexural shear deformations cannot be neglected, even in a simple model.

(e) The rotational inertia in flexure is not insignificant (frequency changes: 2–5%). However, as its influence is concentrated mainly at the extremities, especially the proximal, it can probably be simulated as a concentrated contribution at the proximal extremity.

(f) As one would expect, neglecting the variation in

cross-sectional properties along the tibial axis changes the resonance spectrum. However, bearing in mind that the complexity of the tibial geometry is hereby completely ignored, the changes are remarkably moderate (1-10%). This could be explained if the transverse cross-sections all had nearly equal radii of gyration. In fact, the radii of gyration of compact bone were far from constant. However, if the stiffness of cancellous bone and bone marrow is neglected, it is possible to compute the principal radii of gyration of all three materials in common. It turned out that these radii did not vary much along the tibial axis. Consequently, as far as flexural vibrations are concerned, the human tibia may be viewed as lengthwise much more 'uniform' than its complicated geometry would immediately suggest.

(g) Model (g) differs from model (f) in that: (1) the constant cross-sectional properties used are based on averaging linear dimensions along the shaft, and (2) a point mass simulating cancellous bone at the proximal extremity is added. As shown in Fig. 8, this results in slightly smaller frequency changes than in model (f). More essential however, model (g) is not sensitive to the properties of a single (the middlemost) tibial cross-section, and the point mass necessary to make the model match experiments has its physical counterpart in reality.

In summary, a simplified approach to human tibia flexural vibrations would be to model the tibia as a uniform beam, using meaned cross-sectional properties. Shear deformations should be considered, whereas rotational inertia, axis twist and the stiffness of cancellous bone could be neglected. Bone marrow mass should be included as a uniform distribution, and the mass and rotational inertia at the proximal extremity could both be lumped.

The free vibrations of such a model are mathematically governed by two coupled, ordinary and homogeneous partial differential equations of second order, subject to non-homogeneous boundary conditions. These can be analytically handled by simple means (see e.g. Flügge, 1962), except for the necessarily numerical search for roots in a transcendental frequency equation.

An evaluation of this simple model against experimental data was performed using the material parameters identified in Section 4. The only unknown model parameters were then the mass and rotational inertias of the lumped proximal extremity. These were determined by tuning the simple model to experimental data, using the parameter identification scheme described in Section 4. The natural frequencies of the simple, tuned model then differed from measured frequencies by 0.5–5.0%, the deviations showing no systematic trend. Furthermore, the mode shapes of the simple model and the detailed Finite Element model were almost indistinguishable. While the simple model is treated in full detail (see Thomsen, 1987), it suffices to conclude here that at least the few lowest flexural vibration modes of a human tibia seem to be

reproducible by simple means, without any major loss of accuracy.

Constructing a simple model of human tibia torsional vibrations in this context means constructing a model of about the same level of complexity as the model of flexural vibrations just described. That is, approximating the tibia as a uniform beam, with additional polar moments of inertia concentrated at the extremities. The natural frequencies and mode shapes of this model are easily obtained by standard analytical methods (Flügge, 1962). Two parameters, the polar moments of inertia, are unknown in this model. They were determined by fitting the simple torsional model to the single torsional natural frequency experimentally measured and (simultaneous) to the corresponding mode shape predicted by the Finite Element model. This fitting was successful, in that both natural frequency and mode shape could be accurately matched. However, when it comes to the higher torsional modes, which were not measured but predicted by the Finite Element model, they could not be reproduced. In fact it can be shown, that this simple model is too degenerated to ever represent higher tibial torsional modes in any satisfactory way. [Further details concerning the simple torsional model are given in Thomsen (1987)].

Longitudinal vibrations in the human tibia could probably be modelled too, by means analogous to the simple flexural and torsional models described above, but no attempt was made to do so in this study. As no longitudinal natural frequencies were unambiguously identified through experiments, such a model would be somewhat hypothetical.

6. SUMMARY AND CONCLUSIONS

Free vibrations of an unsupported excised human tibia were studied experimentally and theoretically.

Seven tibial natural frequencies in the range 0–3 kHz were identified experimentally. This was done through structural transfer functions determined by impulse excitation and dual channel FFT-analysis. The seven natural frequencies observed appeared to correspond to three pairs of flexural mode shapes and one torsional mode separating the first two flexural pairs.

The geometry of 38 transverse cross-sections of the tibia were digitized, and the cross-sectional properties of each bone material were computed numerically.

A mathematical model of an excised human tibia was suggested. The tibia was modelled by beam-type Finite Elements, as a straight, twisted, non-uniform Timoshenko beam composed of two linearly elastic and transversely isotropic materials (compact and cancellous bone) and one perfectly flexible material (bone marrow).

Five unknown material parameters in this model were determined by a Bayesian parameter estimation approach. By this, unknown model parameters were

simultaneously tuned until optimal agreement between model predictions and experimental observations were achieved. taking into account experimental uncertainty as well as subjective a posteriori knowledge of unknown model parameters. By the model adaptation. very high model/observation-accordance was achieved by physically realistic parameter estimates.

Using identified model parameters, additional higher tibial natural frequencies could be predicted theoretically. In the range 3–5 kHz, one longitudinal, two torsional and two pairs of flexural natural frequencies were predicted. Two of these frequencies matched noisy peaks in the experimentally determined transfer functions.

Finally, a sensitivity analysis of the Finite Element model confirmed that the human tibia in a vibrational sense can be viewed as much more uniform lengthwise than its complicated geometry would immediately suggest. It was furthermore pointed out that flexural vibrations in the tibia are significantly influenced by shear deformations. In accordance with these findings, two simple tibia models were suggested, based on uniform beam theory with the inclusion of shear deformations and additional non-structural mass contributions. Applied in contexts restricted to the few lowest vibration modes, these simple models will probably be as adequate as the more detailed Finite Element model.

REFERENCES

Bathe, K. and Wilson, E. L. (1976) *Numerical Methods in Finite Element Analysis*. Prentice-Hall, Englewood Cliffs, NJ.
Beck, J. V. and Arnold, K. J. (1977) *Parameter Estimation in Engineering and Science*. Wiley & Sons, New York.
Bendat, J. S. and Piersol, A. G. (1980) *Engineering Applications of Correlation and Spectral Analysis*. Wiley & Sons, New York.
Bourgery, J. M. (1832) *Traite Complet de l'Anatomie de l'Homme*. I. Osteologie, Paris, France.
Buskirk, W. C. van and Ashman, R. B. (1981) The elastic moduli of bone. In Cowin, C. (ed.): *Mechanical Properties of Bone*. ASME Symp., Boulder, Colorado, U.S.A.
Chen, I. I. H. and Saha, S. (1987) Wave propagation characteristics in long bones to diagnose osteoporosis. *J. Biomechanics* 20, 523–527.
Christensen, A. B., Ammitzboll, F., Dyrbye, C., Cornelissen, M., Cornelissen, P. and Perre, G. van der (1986) Assessment of tibial stiffness by vibration test in identification of mode shapes in different supporting conditions. *J. Biomechanics* 19, 53–60.
Collier, R. J., Nadav, O. and Thomas, T. G. (1982) The mechanical resonances of a human tibia: Part I—*in vitro*. *J. Biomechanics* 15, 545–553.
Cornelissen, P., Cornelissen, M., Perre, G. van der, Christensen, A. B., Ammitzboll, F. and Dyrbye, C. (1986) Assessment of tibial stiffness by vibration testing *in situ*—II. Influence of soft tissues, joints and fibula. *J. Biomechanics* 19, 551–561.
Cornelissen, M., Cornelissen, P., Perre, G. van der, Christensen, A. B., Ammitzboll, F. and Dyrbye, C. (1987) Assessment of tibial stiffness by vibration testing *in situ*—III.

Sensitivity of different modes and interpretation of vibration measurements. *J. Biomechanics* 20, 333–342.
Cowper, G. R. (1966) The shear coefficient in Timoshenko's beam theory. *J. appl. Mech.* 33, 335–340.
Dennis, J. E. and Schnabel, R. B. (1983) *Numerical Methods for Unconstrained Optimization and Nonlinear Equations*. Prentice-Hall, Englewood Cliffs, NJ.
Evans, F. G. (1973) *Mechanical Properties of Bone*. Charles Thomas, Springfield, Illinois.
Flügge, W. (1962) *Handbook of Engineering Mechanics*. McGraw-Hill, New York.
Fung, Y. C. (1981) *Biomechanics, Mechanical Properties of Living Tissues*. Springer, Berlin.
Galileo, G. (1638) *Discorsi e Dimostrazioni Matematiche, Intorno a Due Nuove Scienze*. Elsevier, Leiden.
Hight T. K., Piziali, R. L. and Nagel, D. A. (1980) Natural frequency analysis of a human tibia. *J. Biomechanics* 13, 139–147.
Huiskes, R. (1982) On the modelling of long bones in structural analysis. *J. Biomechanics* 15, 65–69.
Huiskes, R. and Chao, E. Y. S. (1983) A survey of finite element analysis in orthopedic biomechanics: the first decade. *J. Biomechanics* 16, 385–409.
I-DEAS GEOMOD (1986). User's Guide, Structural Dynamics Research Corporation, U.S.A.
Khalil, T. B., Viano, D. C. and Taber, L. A. (1981) Vibrational characteristics of the embalmed human femur. *J. Sound Vib.* 75, 417–436.
King, A. I. (1984) A review of biomechanical models. *J. biomech. Engng* 106, 97–104.
Koch, J. C. (1917) The laws of bone architecture. *Am. J. Anat.* 21, 77–298.
Perre, G. van der and Cornelissen, P. (1983) On the mechanical resonances of a human tibia *in vitro*. Letter to the Editor. *J. Biomechanics* 16, 549–552.
Przemieniecki, J. S. (1968) *Theory of Matrix Structural Analysis*. McGraw-Hill, New York.
Sokolnikoff, I. S. (1956) *Mathematical Theory of Elasticity*. McGraw-Hill, New York.
Thomsen, J. J. (1987) Parameteridentifikation i strukturdynamiske modeller af en skinnebensknogle. Ph.D. thesis (in Danish), The Technical University of Denmark.
Viano, D., Helfenstein, U., Anliker, M. and Ruegsegger, P. (1986) Elastic properties of cortical bone in female human femurs. *J. Biomechanics* 9, 703–710.
Wolff, J. (1870) Über die innere architektur der knochen und ihre bedeutung für die frage vom knochenwachstum. *Virchows Arch. path. Anat. Physiol.* 50, p. 389 ff.

APPENDIX

The sensitivity coefficients [equation (10)] were obtained as follows.

The n model resonance frequencies and eigenvectors satisfy [cf. equation (2)]:

$$K\phi_i = (2\pi f_i)^2 \cdot M\phi_i, \quad i = 1, \ldots, n. \qquad (A1)$$

The eigenvectors ϕ_i are normalized, so that:

$$\phi_i^T \cdot M \cdot \phi_j = \delta_{ij} \qquad (A2)$$

where δ_{ij} is the Kronecker delta. Pre-multiplying (A1) by ϕ_i^T, differentiating with respect to a model parameter β_j, using (A2) and the symmetry of K and M in cancelling terms, gives:

$$\frac{\partial f_i}{\partial \beta_j} = \frac{1}{8\pi^2 f_i} \cdot \left(\phi_i^T \cdot \frac{\partial K}{\partial \beta_j} \cdot \phi_i - (2\pi f_i)^2 \cdot \phi_i^T \cdot \frac{\partial M}{\partial \beta_j} \cdot \phi_i \right). \qquad (A3)$$

In our case, the vector of unknown parameters can be written:

$$\beta^T = \{E_q, \rho_r\}, \quad q = 1, 2; \quad r = 1, 2, 3. \qquad (A4)$$

As K is independent of ρ_r, and M is independent of E_q. (A3) gives:

$$\frac{\partial f_i}{\partial E_q} = \frac{1}{8\pi^2 f_i} \cdot \phi_i^T \cdot \frac{\partial K}{\partial E_q} \cdot \phi_i; \quad i = 1, \ldots, n; \quad q = 1, 2 \quad \text{(A5a)}$$

$$\frac{\partial f_i}{\partial \rho_r} = -\frac{1}{2} f_i \cdot \phi_i^T \cdot \frac{\partial M}{\partial \rho_r} \cdot \phi_i; \quad i = 1, \ldots, n; \quad r = 1, 2, 3. \quad \text{(A5b)}$$

K and M are actually obtained by summing individual stiffness and mass matrices of different bone materials:

$$K = \sum_q K_q; \quad M = \sum_r M_r; \quad q = 1, 2; \quad r = 1, 2, 3. \quad \text{(A6)}$$

As E_q appears only in K_q, and ρ_r only in M_r, in both cases as a common factor of all matrix components, we have:

$$\frac{\partial K_q}{\partial E_q} = K_q/E_q; \quad \frac{\partial M_q}{\partial \rho_r} = M_r/\rho_r. \quad \text{(A7)}$$

Inserting (A6) and (A7) in (A5) then gives:

$$\frac{\partial f_i}{\partial E_q} = \frac{1}{8\pi^2 f_i} \cdot \phi_i^T \cdot (K_q/E_q) \cdot \phi_i; \quad i = 1, \ldots, n; \quad q = 1, 2 \quad \text{(A8a)}$$

$$\frac{\partial f_i}{\partial \rho_r} = -\frac{1}{2} f_i \cdot \phi_i^T \cdot (M_r/\rho_r) \cdot \phi_i; \quad i = 1, \ldots, n; \quad r = 1, 2, 3. \quad \text{(A8b)}$$

Thus it is seen that the model sensitivities can be readily computed when the model response (f_i, ϕ_i) is known.

The normalized sensitivities:

$$\bar{f}_{i,j} = \frac{\partial f_i}{\partial \beta_j} \cdot \frac{\beta_i}{f_i}; \quad i = 1, \ldots, n; \quad j = 1, \ldots, p \quad \text{(A9)}$$

become:

$$\bar{f}_{i,E_q} = \frac{1}{2} \frac{1}{(2\pi f_i)^2} \cdot \phi_i^T \cdot K_q \cdot \phi_i; \quad i = 1, \ldots, n; \quad q = 1, 2 \quad \text{(A10a)}$$

$$\bar{f}_{i,\rho_r} = -\frac{1}{2} \cdot \phi_i^T \cdot M_r \cdot \phi_i; \quad i = 1, \ldots, n; \quad r = 1, 2, 3 \quad \text{(A10b)}$$

from which it is clear that the largest sensitivities are associated with the bone material of largest stiffness and mass, that is: with compact bone. Using (A10), (A6), (A2) and (A1), it can further be shown that:

$$\sum_q \bar{f}_{i,E_q} = \frac{1}{2}; \quad \sum_r \bar{f}_{i,\rho_r} = -\frac{1}{2} \quad \text{(A11)}$$

which (as $\bar{f}_{i,E_q} > 0$ and $\bar{f}_{i,\rho_r} < 0$) means that a 1% variation in any of the five unknown model parameters will change the resonant frequencies by at most 0.5%. From (A11) it can also be inferred that the sum of all sensitivities of a given frequency f_i is zero. This has the consequence of making the matrix P defined by equation (11) singular, unless prior information is specified through V_β.